Atmospheric Moisture Transports from Ocean to Land and Global Energy Flows in Reanalyses

KEVIN E. TRENBERTH, JOHN T. FASULLO, AND JESSICA MACKARO

National Center for Atmospheric Research, Boulder, Colorado*

(Manuscript received 26 October 2010, in final form 7 April 2011)

ABSTRACT

An assessment is made of the global energy and hydrological cycles from eight current atmospheric reanalyses and their depiction of changes over time. A brief evaluation of the water and energy cycles in the latest version of the NCAR climate model referred to as CCSM4 is also given. The focus is on the mean ocean, land, and global precipitation P; the corresponding evaporation E; their difference corresponding to the surface freshwater flux $E–P$; and the vertically integrated atmospheric moisture transports. Using the model-based P and E, the time- and area-average $E–P$ for the oceans, $P–E$ for land, and the moisture transport from ocean to land should all be identical but are not close in most reanalyses, and often differ significantly from observational estimates of the surface return flow based on net river discharge into the oceans. Their differences reveal outstanding issues with atmospheric models and their biases, which are manifested as analysis increments in the reanalyses. The NCAR CCSM4, along with most reanalysis models, the exception being MERRA, has too-intense water cycling (P and E) over the ocean although ocean-to-land transports are very close to observed. Precipitation from reanalyses that assimilate moisture from satellite observations exhibits large changes identified with the changes in the observing system, as new and improved temperature and water vapor channels are assimilated and, while P improves after about 2002, $E–P$ does not. Discrepancies among hydrological cycle components arise from analysis increments that can add or subtract moisture. The large-scale moisture budget divergences are more stable in time and similar across reanalyses than model-based estimates of $E–P$. Results are consistent with the view that recycling of moisture is too large in most models and the lifetime of moisture is too short. For the energy cycle, most reanalyses have spurious imbalances of ~10 W m^{-2} within the atmosphere, and ~5–10 W m^{-2} in net fluxes into the surface and to space. Major improvements are needed in model treatment and assimilation of moisture, and surface fluxes from reanalyses should only be used with great caution.

1. Introduction

The strength of the hydrological cycle and its changes over time are of considerable interest, especially as the climate changes. The essence of the overall hydrological cycle is the evaporation of moisture in one place and the precipitation in other places. In particular, evaporation exceeds precipitation over the oceans, which allows moisture to be transported by the atmosphere onto land where precipitation exceeds evapotranspiration, and the runoff flows into streams and rivers and discharges into the ocean, completing the cycle. Changes in moisture storage on land can be significant in the short term, especially in winter in the form of snow, but changes in atmospheric storage are fairly small. Trenberth et al. (2007b, hereafter T07) provided a synthesis of the understanding of the global hydrological cycle and its annual cycle, both globally and for continents.

The global energy cycle is also of considerable interest as it fundamentally changes with increasing greenhouse gases, changes in aerosols, and associated feedbacks. The water cycle is a key part of the energy cycle through the evaporative cooling at the surface and latent heating of the atmosphere, as atmospheric systems play a primary role in moving heat upward. The constraints in the energy budgets at the TOA (all acronyms used in this paper are defined in the appendix), at the surface, and for the atmosphere itself can be used to provide a commentary on accuracy of observational estimates, as in Trenberth et al. (2009). For instance, changes in atmospheric storage

* The National Center for Atmospheric Research is sponsored by the National Science Foundation.

Corresponding author address: Kevin E. Trenberth, NCAR, P. O. Box 3000, Boulder, CO 80307.
E-mail: trenbert@ucar.edu

DOI: 10.1175/2011JCLI4171.1

of energy are limited and the TOA and surface imbalances are therefore very similar, with most of the energy going into or out of the oceans in the form of heat (Trenberth 2009).

The atmospheric conservation of moisture equation when vertically integrated in flux form is

$$\frac{\partial w}{\partial t} + \nabla \cdot \frac{1}{g}\int_0^{p_s} \mathbf{v} q \, dp = E - P, \tag{1}$$

where q is the specific humidity, $w = g^{-1}\int_0^{p_s} q \, dp$ is the precipitable water (total column water vapor), E is the surface evaporation, and P is the net surface precipitation rate. In addition to water vapor, atmospheric liquid water and ice components are also included, although these are mostly small. The whole equation can be expressed also in terms of energy by multiplying by L, the latent heat of vaporization. Frequently the term $Q_2 = L(P - E)$ is referred to as the apparent latent heating arising from the apparent moistening. The use of ''apparent'' is because it includes the small-scale unresolved eddy effects. Because the tendency term is small, the primary balance is thus between the freshwater flux $E - P$ and the moisture divergence.

There have been many estimates of the various components that enter into the hydrological cycle and, in practical applications of Eq. (1), an error term must be considered. Estimates of both E and P separately have considerable uncertainty whether they come from analysis of in situ data, satellite data, hybrid merged products, or comprehensive reanalysis products. Datasets based on the largest global database of river gauge data and a river-routing model provide estimates of the global runoff and discharge of freshwater into the oceans (Dai and Trenberth 2002), and its variability over time from 1948 to 2006 (Dai et al. 2009; see also Trenberth and Dai 2007). Other recent estimates of moisture transports and the overall freshwater discharge from the land to oceans come from Syed et al. (2009, 2010) who used gravity measurements from GRACE to provide better estimates of changes in water storage to complement estimates of $E - P$ from two atmospheric reanalyses (which we show here are deficient) or other datasets discussed in section 2. The other component is the atmospheric moisture transport, which can be assessed at individual radiosonde stations (e.g., Rosen and Omolayo 1981), or through atmospheric analyses. van der Ent et al. (2010) provide new estimates of the movement of atmospheric moisture and how much is recycled in various regions. A brief review of some of the datasets is provided in section 2, although we rely on the synthesis performed by T07 as a basis for some of the comparisons here.

The focus of this paper is assessing the capabilities of recent modern atmospheric reanalyses based on four-dimensional data assimilation to provide reliable estimates of the vertically integrated moisture transports and other components of the hydrological cycle. As a complementary component, an assessment is also made of the global mean energy budget and flows of energy through the climate system in reanalyses, and how they compare with the observationally based assessment of Trenberth et al. (2009). The ability of radiosondes to measure water vapor accurately has improved over time (Dai et al. 2011), but spatial gaps and missing data are always an issue. Accordingly, reanalyses provide a synthesis of all available data and can bias correct for errors in radiosondes. Indeed, tremendous strides have been made in the ability to measure atmospheric moisture from satellites so that moisture fields have greatly improved in reanalyses, especially over the ocean. These fields have also been helped by the assimilation of radiances directly. Nonetheless, there are continual changes over time in the observations that lead to large spurious apparent changes in the fields and affect the hydrological cycle in the assimilating models.

Moreover, the moisture budget is generally not closed in reanalyses owing to the analysis increment arising from errors in the state variable fields and observational uncertainties, and also a very small term that represents a negative filling to ensure that values of q and w are positive definite. Effectively another term exists on the right-hand side of Eq. (1) in the reanalysis moisture budget (e.g., Bosilovich et al. 2011). A step forward in recent reanalyses is the use of either a four-dimensional data assimilation system for ERA-I (e.g., Simmons et al. 2010), or an incremental analysis update technique for MERRA (Bloom et al. 1996), both of which allow the analyzed fields to evolve smoothly in time instead of with jumps at times of analyses, and this has a major advantage of largely eliminating the spinup problem of the hydrological cycle. Accordingly, we will focus on these two reanalyses in the moisture budgets assessed here. Nonetheless, in spite of major advances in bias corrections for changes in the observing system over time (Dee and Uppala 2009), there have been substantial changes in observations, noted below, that affect the quality of the atmospheric analyses of temperature and water vapor quantities.

Of particular note are the introduction of the SSM/I observations in mid-1987, the advances made in going from TOVS to ATOVS, along with the AMSU-B water vapor channels from late 1998 (*NOAA-15* replaced *NOAA-12*) to 2001 (*NOAA-16* replaced *NOAA-14* on 20 March), the AIRS observations in about late 2002, and the GPS RO measurements from about 2002 on, increasing in volume after COSMIC was launched in April 2006.

The capabilities of new modern atmospheric reanalyses, summarized by Trenberth et al. (2011), to deal with moisture fluxes and global energy are assessed here. In particular, it is possible to use the E and P from reanalyses to derive 1) a value of $E - P$ over the ocean, 2) a value of $P - E$ over land, and also to use the analyses to estimate 3) a value for the transport of atmospheric moisture from ocean to land. Another independent estimate (from Dai and Trenberth 2002; Dai et al. 2009) is 4) the value of the return flow in rivers and at the surface. Ideally these four estimates are identical for averages (where the storage tendency is small) but, in practice, they are not. In reanalyses, differences among the first three estimates arise from the analysis increment, which precludes reanalyses from satisfying physical closure constraints in either the energy or water cycles, and indeed they are not satisfied. Moreover, specified sea surface temperatures (SST) in the reanalyses provide an ''ocean'' that has infinite heat and water capacity to take up or provide energy or water to the atmosphere. The degree to which the reanalyses satisfy the physical constraints and the extent of the imbalances provides a useful commentary on the quality and usability of the reanalyses for many purposes.

Section 2 discusses the observational datasets that provide information for evaluating the reanalyses. Section 3 introduces the current atmospheric reanalyses. The water-cycle-related quantities are addressed in section 4 and the energy cycle in section 5. A brief analysis of the NCAR CCSM4 is given from these perspectives in section 6 both to highlight the values in a state-of-the-art climate model and to illustrate the difference of working in a closed system that conserves water and energy, as opposed to the reanalyses that do not.

2. Estimates of hydrological cycle components

a. Precipitation

The lack of ground-based measurements of precipitation has meant that most estimates are based on various algorithms applied to satellite data, perhaps merged into synthesized products such as the GPCP (Adler et al. 2003; Huffman et al. 2009) and the CMAP (Xie and Arkin 1997). Comparisons of these datasets and others (Adler et al. 2001; Yin et al. 2004; Smith et al. 2008) reveal large discrepancies over the ocean; and over the tropical oceans mean amounts in CMAP and GPCP differ by 10%–15%. As noted by Trenberth et al. (2007a), calibration using observed rainfall from small atolls in CMAP was extended throughout the tropics in ways that are now recognized as incorrect, while GPCP is biased low by 16% at such atolls (Adler et al. 2003). The temporal sampling limitations from two instantaneous precipitation rates per day from polar orbiters are offset by geostationary satellites, but with less-accurate infrared sensors.

Some advances occurred with the TRMM satellite mission, which allowed comparison of various measurement techniques such as TRMM precipitation radar and passive TMI. However, Robertson et al. (2003) documented poorly correlated behavior (correlation 0.12) between the monthly, tropical ocean-averaged precipitation anomalies from the PR and TMI sensors. The TRMM PR has uncertainties resulting from microphysical and beam-filling assumptions.

A comprehensive summary of observed changes in precipitation is given in the IPCC Fourth Assessment (Trenberth et al. 2007a), and updated in Trenberth (2011). Schlosser and Houser (2007) and Wentz et al. (2007) provided estimates of precipitation and their trends. However, the precipitation and evaporation estimates of Schlosser and Houser (2007) are out of balance and reveal likely spurious changes over time associated with changes in satellites. Gu et al. (2007) documented global and tropical rainfall changes using the GPCP and found near-zero global changes but with large variability and changes over land that are largely compensated for by opposite changes over the oceans. This is especially the case for El Niño events (Trenberth and Dai 2007). An update of the Gu et al. analysis (also Huffman et al. 2009) confirms that there are no significant trends since 1979. This is in marked contrast to Wentz et al. (2007) who found a significant upward trend from 1987 to 2006, but that result depended critically on the time period and the dataset used.

The precipitation fields in atmospheric reanalyses leave much to be desired (Trenberth and Guillemot 1998; T07; Bosilovich et al. 2008) but in the high-latitude extratropics, where remote sensing is much less reliable, studies have shown that the oceanic satellite estimates are less accurate when compared with reanalysis data and a new precipitation dataset called MSAP tries to take advantage of this (Sapiano et al. 2008).

The assessment by T07 examined only the precipitation datasets, while Trenberth et al. (2009) assessed the precipitation latent heating in the context of closure of the total energy cycle. The latter suggests values somewhat higher than GPCP values as do new measurements from *CloudSat* (e.g., Stephens and Haynes 2007), and by using the CMAP ocean values in lower latitudes Trenberth et al. (2009) provide a justification for overall ocean values being higher by 5.7% than the GPCP values, and therefore 3.34 mm day^{-1} for the ocean. Globally the 2.63 mm day^{-1} for GPCP was increased by 5% to 2.76 mm day^{-1} for the 2000–04 period. The monthly temporal variability (95%) from GPCP is $\pm 0.6\%$, while the structural uncertainty is more like $\pm 5\%$.

b. Evaporation

Despite the substantial uncertainties in precipitation, even greater uncertainties lie in the estimates of evaporation because it is seldom measured, and instead is estimated from bulk flux formulas. While patterns and general amounts are not unreasonable, systematic biases are substantial. Satellite-based products involve extra uncertainties because the surface variables required for a bulk flux formulation have to be estimated from finite layer values of moisture and temperature, and they also suffer from biases, which can change substantially over time as satellite instruments change (Schlosser and Houser 2007). The HOAPS, based on SSM/I data, provides turbulent fluxes, and the latest HOAPS-3 update (see online at http://www.hoaps.zmaw.de/) covers the period from 1987. Daily and monthly products of latent heat fluxes at 1° resolution provided by the GSSTF data (Chou et al. 2003, 2004) have been updated in 2010.

Surface fluxes from in situ data have typically exhibited large systematic biases as seen when integrated over the global ocean. The NOC1.1 climatology (Josey et al. 1999) in which observational metadata were employed to correct individual observations featured an imbalance of the net surface flux over the oceans with an underestimation of the ocean heat loss of ~30 W m^{-2}. A subsequently improved product (NOC1.1a) made adjustments to achieve closure of the global budget to within 2 W m^{-2} (Grist and Josey 2003); however, this approach has its own problems as the adjusted fluxes no longer showed agreement with some research buoy measurements, indicating that the adjustments lacked correct spatial structure. A new version of the climatology (Berry and Kent 2009, 2011), termed NOC2.0, provides for error estimates for all of the basic meteorological and derived flux fields using optimal interpolation of daily estimates of ship data and spans the period 1973–2006.

The OAFlux product (Yu and Weller 2007) has been produced by combining several reanalysis (R1, R2, and ERA-40) and satellite datasets using a variational approach with monthly fields beginning in 1958, although the data input for blending before 1985 consisted only of reanalysis variables. Subsequent evaluation revealed good agreement with in situ buoy data. The Large and Yeager (2009) hybrid flux dataset has gone through several versions. From an energy-budget closure evaluation (Trenberth et al. 2009) standpoint, the calibrated OAFlux product appeared to be best of those available for evaporation, although the validity of trends is in question.

Over land, the evapotranspiration (ET) estimates also suffer from difficulties although there are now over 250 flux towers with point measurements that have been used to tune estimates, such as from Jung et al. (2010). They find ET to be 65×10^3 km^3 yr^{-1} from 1982 to 2008, similar to previous estimates summarized by Oki and Kanae (2006) of 65.5×10^3 km^3 yr^{-1}.

c. Observational estimates used

T07 presented estimates of the mean annual cycle of the atmospheric hydrological cycle based on 1979–2000 data from multiple sources. These include monthly estimates of P, E, atmospheric moisture convergence over land, and changes in atmospheric storage, for the major continental landmasses, zonal means over land, hemispheric land means, and global land means. A new annual mean global hydrological cycle was presented and will be the main basis for evaluating the reanalysis results, as modified below to apply to the 2000s. The units given for the exchanges are integrated values taking the area into account and are 1000 km^3 yr^{-1}, which is the same as Eg yr^{-1} (1 Eg = 10^{18} g). This unit corresponds to 0.0317 Sv (Sv = 10^6 m^3 s^{-1}), or alternatively, 1.0 Sv corresponds to 31.56 of these units or 0.17 mm day^{-1} globally.

Based on streamflow discharge into the ocean (Dai and Trenberth 2002; Dai et al. 2009) the moisture transport from ocean to land is 40×10^3 km^3 yr^{-1}. These values include crude estimates for Antarctica (2.6×10^3 km^3 yr^{-1}), so the rest of land value is ~37.3×10^3 km^3 yr^{-1} overall. For the 1990s, when the impact of Mount Pinatubo dropped values down somewhat owing to reduced solar flux (Trenberth and Dai 2007), the estimate is ~39×10^3 km^3 yr^{-1}. The uncertainties in these estimates are not well determined. The temporal variability from 1948 to 2004 has a standard deviation of 0.98×10^3 km^3 yr^{-1} giving an uncertainty in a decade mean of about $\pm 0.6 \times 10^3$ km^3 yr^{-1} (2 standard errors). However the structural uncertainty is likely much larger, perhaps 10%.

For the global hydrological cycle (in Fig. 9) presented below, the values from T07 for 1979–2000 are used as background values but modified to apply to the 2002–08 period and take newer datasets into account. The GPCP version 2.1 gives values of global P of 2.67 mm day^{-1} for the 1990s and 2.68 mm day^{-1} for 2002–08, slightly higher than the values used in T07 (see Huffman et al. 2009). For the ocean these are 2.91 mm day^{-1} for the 1990s and 2.92 mm day^{-1} for 2002–08; while for land the values are 2.09 and 2.10 mm day^{-1}, respectively. Accordingly, rather than the 373×10^3 km^3 yr^{-1} for ocean precipitation in T07, GPCP for 2002–08 are 386, while the values in Trenberth et al. (2009) are 1.8% higher (392). For land, the precipitation value is 114×10^3 km^3 yr^{-1} (instead of 113), and evapotranspiration is 74×10^3 km^3 yr^{-1}. This is much larger than the recent values by Jung et al. (2010), but the latter do not account for wetlands, inland

TABLE 1. Summary of the main atmospheric reanalyses that are current, with the horizontal resolution (latitude; T159 is equivalent to about 0.8°), the starting and ending dates, the approximate vintage of the products, and the current status.

Reanalysis	Horizontal resolution	Dates	Vintage	Status
NCEP–NCAR R1	T62	1948–present	1995	Ongoing
NCEP–DOE R2	T62	1979–present	2001	Ongoing
CFSR (NCEP)	T382	1979–present	2009	Ongoing
C20r	2°	1871–2008	2009	Done
ERA-40	T159	1957–2002	2004	Done
ERA-I	T255	1989–present	2009	Ongoing
JRA-25	T106	1979–present	2006	Ongoing
MERRA (NASA)	0.5°	1979–present	2009	Ongoing

lakes or seas, and the like, and their value of 65×10^3 km^3 yr^{-1} is not viable in the global context.

For the global energy cycle (in Fig. 10), the Trenberth et al. (2009) figure estimates for the 2000–05 period is used as background. The reanalysis values plotted are for 2002–08, as this interval follows the major updates to the satellite-based observing system.

3. Atmospheric reanalyses

Atmospheric reanalyses have been produced by the major meteorological centers [NCEP (NOAA), ECMWF, JMA, and NASA]. Several new reanalyses have recently become available, and those currently ongoing are given in Table 1 along with ERA-40, with the resolution and dates covered.

a. Early-generation reanalyses

The first generation of atmospheric reanalyses in the mid- to late 1990s at NCEP (Kalnay et al. 1996) called NCEP–NCAR, or R1, had substantial problems that limit their use, particularly for global climate change and variability studies. A second limited version of the NCEP reanalysis (called NCEP–DOE or R2) was run to address some problems (Kanamitsu et al. 2002) but is still a first-generation reanalysis.

An earlier analysis of moisture transports used the R1 reanalyses (Trenberth and Guillemot 1998) and their extension to current times. The first-generation NCEP reanalyses did not use SSM/I data or water vapor channels and, hence, had no information on moisture over the oceans. The result is that the ocean moisture fields are largely model values that are severely deficient in spatial and temporal variability and lead to transports onshore that are mostly too low (Trenberth et al. 2005). The NCEP model moisture budget was shown not to balance (this is associated with the increments in the assimilation), as is true of reanalyses generally. Jiang et al. (2005) noted problems with earlier reanalysis surface fields and surface fluxes.

Two second-generation global reanalyses, the ERA-40 (Uppala et al. 2005) and the JMA 25-yr reanalysis (JRA-25) (Onogi et al. 2007), addressed some of the shortcomings of the earlier reanalyses, but many of the problems tied to observing system changes and model deficiencies remain. Trenberth et al. (2005) evaluated precipitable water from NCEP reanalyses, ERA-40, and SSM/I, and identified spurious variability in all reanalyses, with only SSM/I providing reliable trends over the ocean. Other evaluations of NCEP reanalyses by Smith et al. (2001) and Sturaro (2003), and ERA by Sterl (2004) highlight problems in continuity and quality. T07 computed the monthly vertically integrated atmospheric water and energy components, the transports, and their divergences and generated the diabatic heating and $E - P$ from the moisture budget. Substantial problems were again revealed in the ERA-40. Trenberth et al. (2011) provide other examples of problems in quality and homogeneity of the basic observations, bias corrections, spurious trends and variability, spinup of the hydrological cycle, and problematic surface flux and stratospheric fields.

b. Current reanalyses

A new reanalysis of the atmosphere, ocean, sea ice and land over 1979–2009 has been produced by NCEP under a project referred to CFSR (Saha et al. 2010). There are three main differences from R1 and R2: 1) much higher horizontal and vertical resolution [T382L64 (about 35 km) vs T62L28] with sigma–pressure hybrid levels; 2) the guess forecast is generated from a coupled atmosphere–ocean–sea ice–land system; and 3) radiance measurements from the historical satellites are assimilated. The oceanic reanalysis has the first guess provided by CFS. It has 40 levels in the vertical to a depth of 4737 km, and a high horizontal resolution of 0.25° in the tropics, tapering to a global resolution of 0.5° poleward of 10°N/S. Because the archive available is on 37 pressure levels, vertical integrals contain noise from the inaccurate lower-layer treatment (Trenberth et al. 2002). Also we have discovered a number of problems in the CFSR reanalyses and, for the computations given here, the problem days were simply excluded.

JMA has started a new reanalysis that is not yet available. ECMWF is producing ERA-I, a global reanalysis of the data-rich period since 1989 (Simmons et al. 2007; Dee et al. 2011). Relative to the ERA-40 system, ERA-I incorporates many important model improvements such as resolution and physics changes, the use of four-dimensional variational (4D-Var) data assimilation, and various other changes in the analysis methodology. MERRA (Bosilovich et al. 2006; 2011) is a new reanalysis from NASA Goddard from 1979 to the present based on a new version of the data assimilation system (GEOS-5) and the NCEP unified gridpoint statistical interpolation analysis scheme. The model resolution of MERRA is 0.667° longitude by 0.5° latitude with 72 levels extending to a pressure of 0.01 hPa. MERRA provides various quantities that are used to calculate $E - P$ as well as moisture transport, without going through the mass-correcting procedure that is necessary in the other reanalyses, and is possible because MERRA uses the incremental analysis update procedure that evolves the fields smoothly.

A different kind of reanalysis, the C20r for the entire twentieth century and beyond, based on specified SSTs and analysis of surface or sea level pressures has been performed with the ensemble Kalman filter (Compo et al. 2011), using a recent data assimilation system. Because data are assimilated only at the surface, the atmospheric increments affect the free atmosphere indirectly in this reanalysis. The full moisture budget has not (yet) been computed for R2, CFSR, and C20r.

Bosilovich et al. (2011) have also carried out a comprehensive evaluation of the current reanalyses in parallel with a focus on MERRA and the global energy and water cycles.

4. The hydrological cycle

a. Precipitation, atmospheric moisture, and freshwater transport

As a result of the changes in the observing system, noted above, the precipitation produced in reanalyses is not stationary and exhibits large spurious trends. An example is given in Fig. 1 of the MERRA and ERA-I precipitation compared with estimates from GPCP, version 2.1. The GPCP values are quite stable and have no significant trends, with the main variations corresponding to El Niño fluctuations (Gu et al. 2007; Huffman et al. 2009). Over land the strong annual cycle is evident and values are closely matched by ERA-I, although the latter are slightly higher in the 1990s. MERRA land values are biased low until about 2001 after which they match the observations quite well. Over the ocean, large spurious trends (~10% decade^{-1}) exist in MERRA values until about 2001 when an annual cycle also emerges. As noted by Bosilovich et al. (2011), the spurious trends arise from the TOVS to ATOVS transitions from 1998 to 2001.

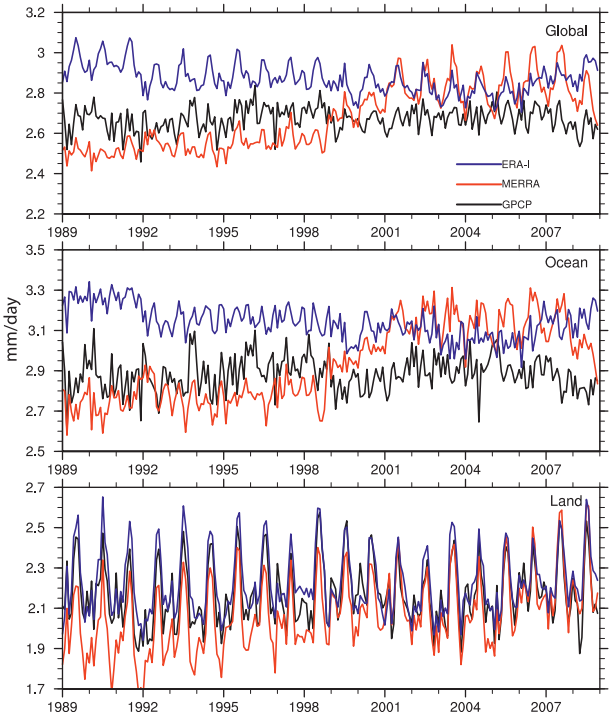

FIG. 1. Time series of (a) global, (b) ocean, and (c) land precipitation (mm day^{-1}) from MERRA (red), ERA-I (blue), and GPCP (black).

ERA-I ocean values reveal an abrupt drop in January 1992, and slightly lower values with a less distinct annual cycle after 1999. These arise from changes in observations from SSM/I as new DMSP satellites came online in January 1992 to allow retrieval of total column water vapor from rain-affected radiances. Increases in SSM/I observations by an order of magnitude in 1992, were followed by further increases in 1999 and 2000, but then major decreases in late 2006 and 2008 as instruments failed. Because of an implementation error in the assimilation of rain-affected radiances in ERA-I, increased numbers of SSM/I observations tended to dry out the atmosphere somewhat, and this effect gradually reverted when the number of observations decreased in 2006 and 2008 (D. Dee, 2010 personal communication; also Dee et al. 2011). Values are ~10% or higher than GPCP values throughout the record.

There is no obvious relationship among the three sets of values over the ocean. Consequently, in the global mean there are also trends in MERRA, and values appear to be more stable after 2001 in both sets of fields. The values after 2001 are also more compatible with our adjusted GPCP values (increased by 5.7% over the ocean) and with estimates of river discharge.

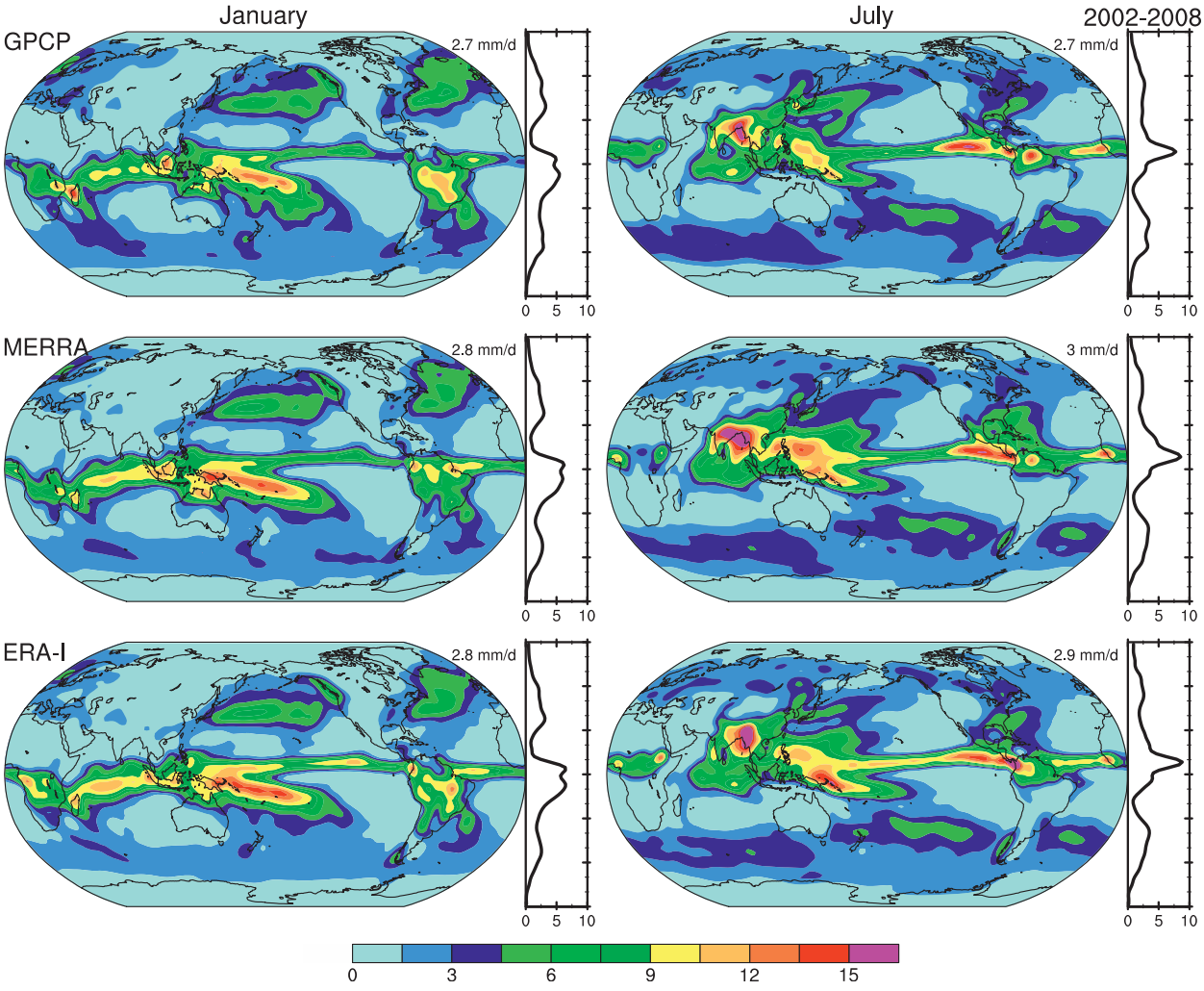

FIG. 2. Maps of precipitation (mm day^{-1}) for (left) January and (right) July for (top) GPCP, (middle) MERRA, and (bottom) ERA-I for 2002–08. Values at top-right of each panel are global means, and zonal means are given to the right of each panel.

Maps of the mean precipitation for January and July from 2002 to 2008 for GPCP, MERRA, and ERA-I (Fig. 2) show strong similarities, with the climatological convergence zones and monsoon rains well represented. Differences are most apparent in July, and MERRA appears to be deficient in the mei-yu–baiu rains east of Japan. In general the quality of the reanalyses is high, and much higher than in older reanalyses. Nevertheless, there are important differences with observations including in well-observed areas, such as central North America in summer. Large errors occur in central Africa in MERRA in July (discussed below) and substantial differences are evident in the southern Amazon in January between GPCP and both MERRA and ERA-I (see also Fig. 7 below).

A key component of the precipitation is the moisture field, and Fig. 3 presents the total atmospheric column water as the vertical integral for MERRA, ERA-I, and their differences for 2002–08. The precipitable water is the dominant component of this field. It reveals quite large systematic differences between the two reanalyses, with higher precipitable water over the ocean in MERRA but lower amounts in interior Africa, South America, and southern Asia in the vicinity of the Himalayas. Differences are greatest in the summer hemisphere, when mean values are larger. The time series of the total column water (Fig. 4) shows ERA-I values to be relatively high prior to 1992 over both land and ocean. Over the ocean, we have compared with independent SSM/I values, which agree quite well with ERA-I prior to 1992 and MERRA values after about 2000. ERA-I ocean values appear to be low after 1992.

The differences between January and July mean vertically integrated moisture transports for the same period, as given by MERRA and ERA-I (Fig. 5), highlight the

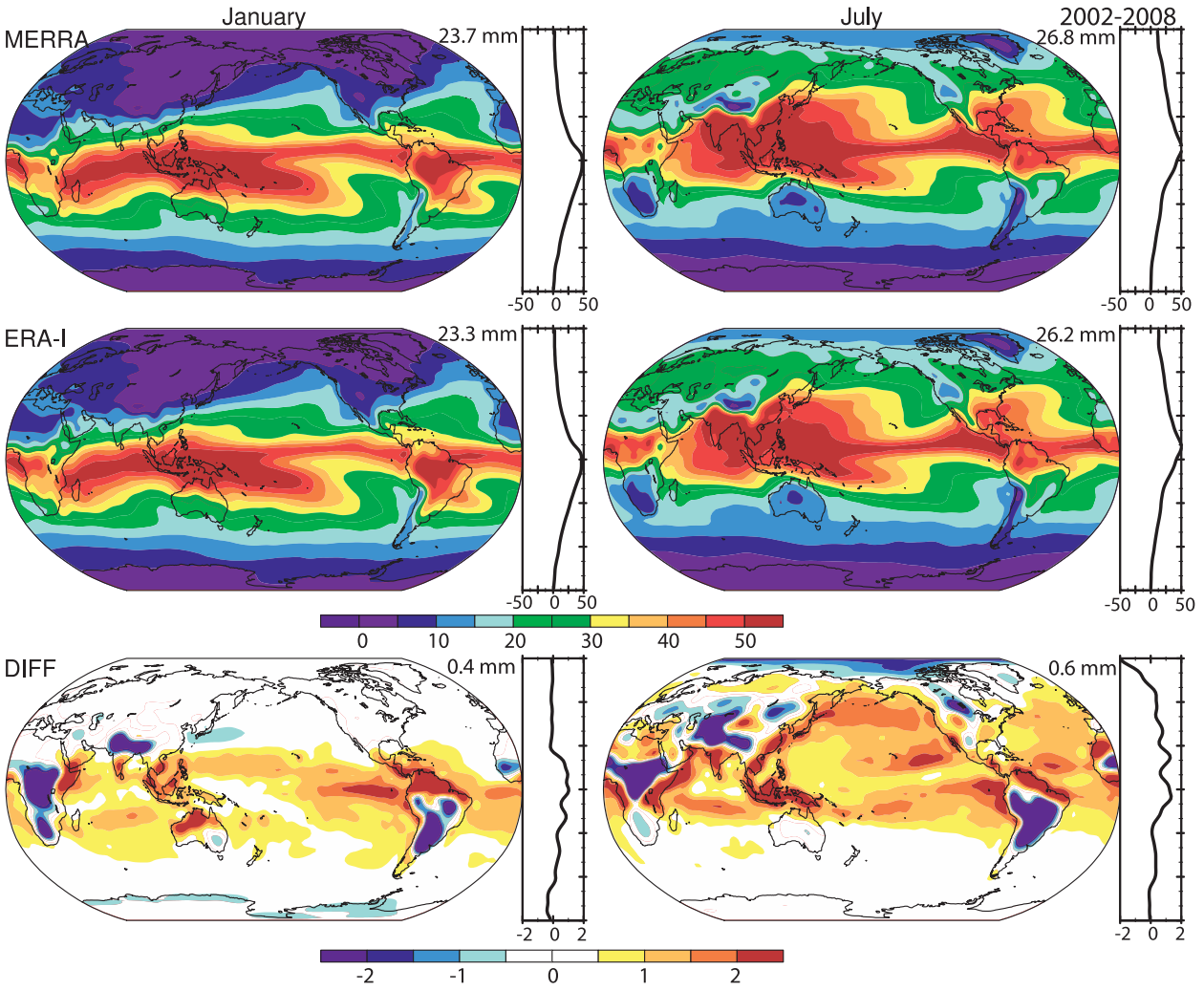

FIG. 3. Maps of total column atmospheric water for (left) January and (right) July for (top) MERRA and (middle) ERA-I, and (bottom) their difference (mm) for 2002–08.

low-level moisture transports in monsoon circulations. The main differences between the two products (Fig. 5) are in low latitudes where MERRA has much stronger trade wind transports mainly because of the larger atmospheric moisture amounts (Fig. 3). These differences are substantial when compared with expected changes over time. It is then straightforward to compute the divergence of these transports. We also compute the tendency term [see Eq. (1)], but the latter is very small for time averages. The resulting $E - P$ field (Fig. 6) has similar overall features to those published elsewhere, with major source regions for atmospheric moisture in the subtropical anticyclones, and major sink regions where $P > E$ in the convergence zones and summer monsoon rains. The ocean storm tracks show up clearly. Differences in $E - P$ are much more apparent than in the transports, especially in July. Throughout the tropics the differences often exceed 1 mm day^{-1}, which can be 20% of the total.

The annual mean $E - P$ can be revealing over land where it is negative in nature, as runoff is positive definite, except where there are sources of surface water such as in lakes or inland seas. The annual means for 2002–08 for MERRA and ERA-I from the moisture budget (Fig. 7) show several areas that potentially violate this physical constraint on land. For instance, for the whole of Australia the value for $E - P$ is positive (Table 3 given below) for ERA-I but is appropriately negative for MERRA, and spurious positive values occur near all coasts (Fig. 7). The interior of South America east of the Andes and central Africa, however, are areas with major problems in MERRA, and parts of Africa and South America are also clearly in error in ERA-I although to a lesser extent. The central African problem in MERRA was identified

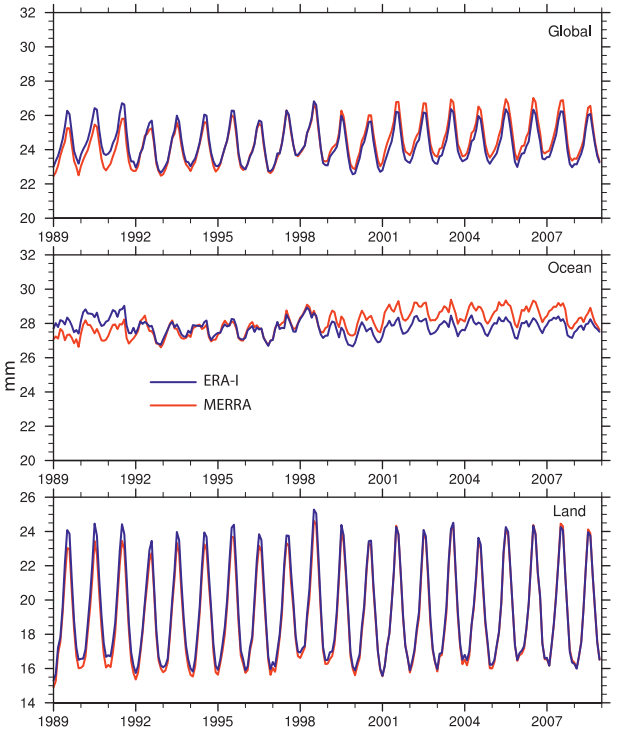

FIG. 4. Time series of (top) global, (middle) ocean, and (bottom) land total column atmospheric water (water vapor, liquid, and ice) (mm) from MERRA (red) and ERA-I (blue).

by Bosilovich et al. (2011) as due to an erroneous radiosonde station that was not rejected by the quality control, unlike in ERA-I. Both ERA-I and MERRA monsoon precipitation are also too low in the southern Amazon in January (Fig. 2). Even in central North America there are positive values in both reanalyses (Fig. 7), which arise mainly in summer. This could be possible if irrigation and withdrawal of aquifer waters were large, but comparison with GPCP reveals that the summer precipitation is too low in both reanalyses (Fig. 2). Problems are also evident over India in ERA-I (Fig. 7), traceable to the precipitation field (Fig. 2). However, inland seas such as the Caspian and Aral Seas are revealed as important sources of moisture.

b. *The global water cycle: Comparisons among reanalyses*

By averaging fields separately over land and ocean, a result that depends somewhat on the grid size and the land–sea mask, the net transport of moisture from ocean to land is computed. Care has been taken to ensure the fraction of land and ocean remains the same in different grids. However, for Fig. 8 (given later), values were computed on the native model grid with appropriate area weighting. Some errors arise because of the poorer representation of coastlines and orography in low-resolution reanalyses (especially R1 and R2) and, when coastal ranges are too smoothed, the advection of moisture onshore can be excessive. Because changes in storage of moisture in the atmosphere are small, the estimated average value of $E - P$ over the ocean should be the same as $P - E$ over land, and the same as the measured transport from ocean to land. Note that the global mean of the divergence field is identically zero.

Table 2 provides the annual mean and monthly mean values of the net transport of atmospheric moisture from ocean to land from the moisture budget for the 1990s, expressed as $P - E$ over land, for which the "observed" annual value is 0.71 mm day^{-1}, corresponding to 39×10^3 km^3 yr^{-1}. Values greater than this amount occur in the northern winter, with strong contributions from the South American monsoon rains in the Amazon (Fig. 6). Although precipitation is generally largest in July and August over Northern Hemisphere land, so too is the evapotranspiration, especially in North America (T07). Table 2 also suggests that the reanalyses that are low for the annual mean are biased low year-round.

Time series of $E - P$ from model values for the globe and ocean domain and $P - E$ for land are given in Fig. 8 along with the computed transport from ocean to land. The latter is fairly stable over time and shows good agreement among the reanalyses that we have examined, although only ERA-I and MERRA are included in the figure. In contrast, the fluctuations in the model-based values are substantial in response to the changes in the observing system, and discrepancies among reanalyses can be huge (Fig. 9). Only ERA-I seems relatively immune from big changes after 1998, although it is affected by changes in SSM/I data.

The results from all of the available reanalyses for the main atmospheric components of the hydrological cycle are given in Fig. 9 for 2002–08. All P-ocean estimates are high relative to the T07 estimate or GPCP (386); MERRA, R1, and ERA-I values are within 7% while JRA, R2, ERA-40, CFSR, and C20r are clearly excessive. Aside from MERRA, E-ocean from reanalyses are also high when compared with the estimated values from T07, and JRA, R2, CFSR, and C20r are clearly much too high, even allowing for uncertainties or adjustments in observed estimates.

As noted above, the older NCEP reanalyses contain limited moisture information over the ocean and the moisture fields are largely model values. For MERRA, ERA-40, and CFSR (Fig. 9), P exceeds E over ocean, a result that cannot be physically correct, highlighting the fact that the moisture for precipitation comes from the analysis increment and is then precipitated out (T07). These models were evidently not capable of holding the observed levels of moisture, and promptly activated

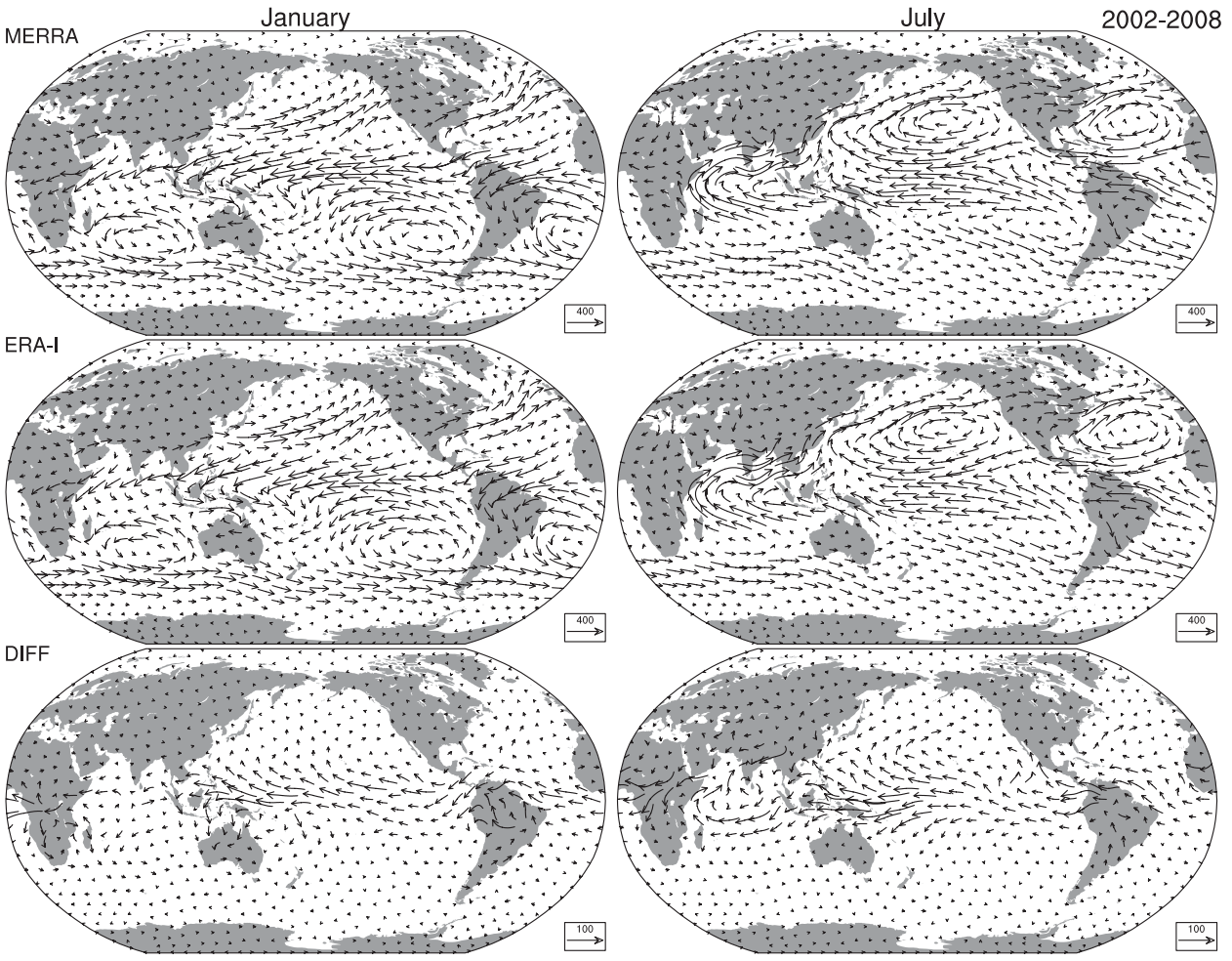

FIG. 5. Vertically integrated moisture (including liquid and ice; kg m^{-1} s^{-1}) transports for 2002–08 from (top) MERRA and (middle) ERA-I, and (bottom) their difference for (left) January and (right) July. The vector key is given to the lower-right of each panel and is a factor-of-4 smaller for the differences.

convective parameterization that gets rid of the excess. This is evidently also true for R2 once the transport onto land is taken into account. Big changes in ERA-I versus ERA-40 are evident.

Transport of moisture onto land from the moisture budget (Fig. 9) is less than $E - P$ for the ocean in JRA and R1, suggesting that some precipitation occurs prematurely in the models over the oceans, while MERRA is the same, CFSR is slightly higher, and ERA-I is slightly less than the river discharge estimate.

On land, aside from JRA, which is low, precipitation is generally close to observed values, presumably because this quantity is tuned to match observations to some degree. For CFSR on land the analysis increment evidently supplies some moisture for precipitation as evapotranspiration is slightly low compared with the estimate of 74, while precipitation is unduly high (Fig. 9). The E is high for MERRA, R1, R2, and C20r on land. As a result, over land $P - E$ is generally too low except for C20r, while CFSR is much too high. Hence, there is a rough balance between the onshore transport and land $P - E$, with largest differences for MERRA and CFSR.

There are quite substantial changes for 2002–08 versus the 1990s in P-ocean, for MERRA a 12% increase, but for ERA-I a 4% decrease (Fig. 1). Evaporation is similar between time periods for both land and ocean although very different for the ocean between the two reanalyses. The P changes have a major adverse effect on $E - P$ for MERRA whose value drops to near zero. In contrast, ERA-I values jump after about 1997 owing to a modest decrease in P and an increase in E. Land precipitation increases by 6% for MERRA (see Fig. 1) and $P - E$ over land is increased by 15% for 2002–08. A slight increase occurs for ERA-I as well. The land values are more stable overall, signifying the more stable observing system over land, where radiosondes control values. The actual

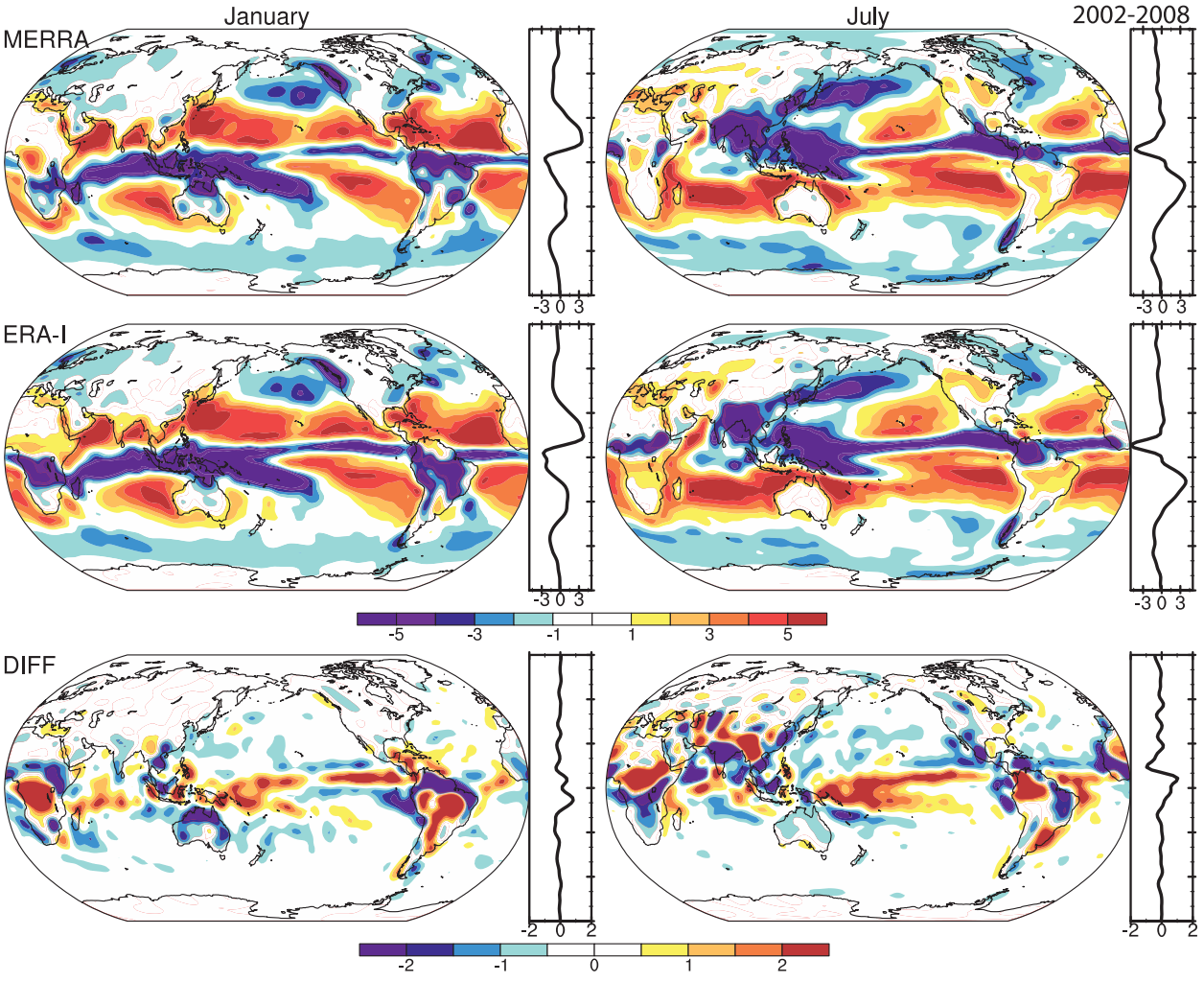

FIG. 6. The $E - P$ (mm day^{-1}) computed from vertically integrated atmospheric moisture budgets in reanalyses from (top) MERRA and (middle) ERA-I, and (bottom) their difference for (left) January and (right) July for 2002–08. Note: the color scale for the bottom panels is half that of the top four; at the right of each panel is the zonal mean.

transport from ocean to land is much more consistent between the two reanalyses (Fig. 8) although there are increases from the 1990s to 2002–08. Large abrupt jumps occur in JRA and CFSR in the hydrological cycle in late 1998 (not shown) in association with the changes in the observing system from TOVS to ATOVS. For CFSR, the global $E - P$ decreases from about -0.2 to -0.4 mm day^{-1} after October 1998, somewhat comparable to MERRA in Fig. 8, but also indicating a severe imbalance in the hydrological cycle.

To examine the source of some of the discrepancies in more detail, the contributions of the individual landmasses to the total land moisture budget are briefly explored, and compared with T07 results based on modeling the land runoff and evaporation using a land surface model forced with observed forcings (precipitation, clouds, temperatures, atmospheric moisture, etc). The river discharge was estimated as the residual, instead of using observed river flow in Dai and Trenberth (2002) and Dai et al. (2009). In the reanalyses in Table 3, the continents mostly consist of just the contiguous land, except that Tasmania is included in Australia, and Newfoundland is included in North America, but islands to the north of mainland Canada are not included and other islands are also treated separately. In that regard there are some differences with T07 and Dai and Trenberth (2002), which included Greenland with North America.

One source of bias for the onshore moisture transports is the contribution from Antarctica, which ranges from 1.1 to 2.7 ($\times 10^3$ km^3 yr^{-1}) in the different reanalyses (vs the T07 estimate of 2.6×10^3 km^3 yr^{-1}), although the higher-resolution ERA-I and MERRA values are 2.1 and 2.4 ($\times 10^3$ km^3 yr^{-1}), respectively (about 0.4 mm day^{-1} for the whole of Antarctica). The

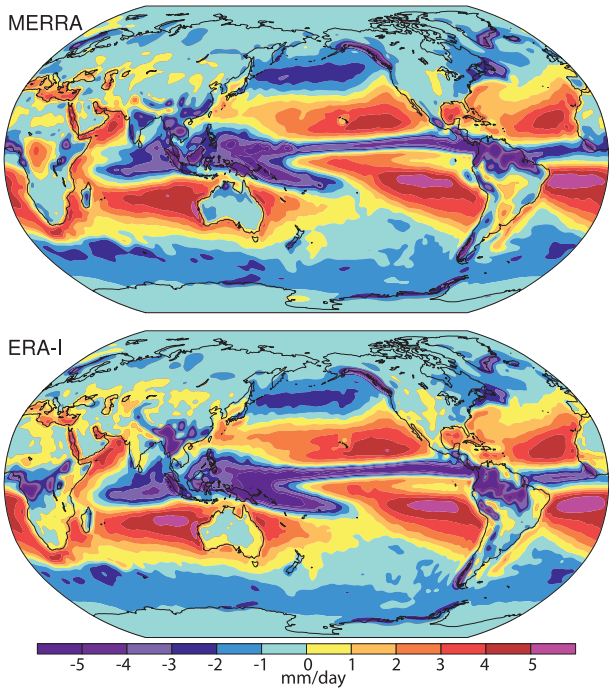

FIG. 7. Annual mean $E - P$ (mm day^{-1}) from (top) MERRA and (bottom) ERA-I for 2002–08 computed from the atmospheric moisture budget.

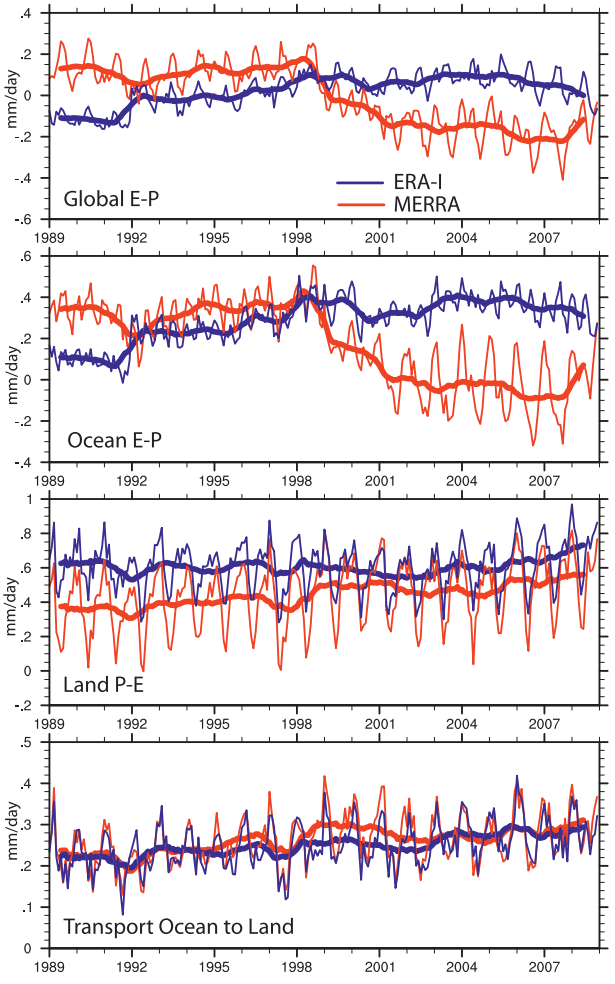

FIG. 8. Time series for MERRA and ERA-I of values of $E - P$ based on the model values for (top) global and (top middle) ocean, and (bottom middle) $P - E$ for land; as well as (bottom) the net transport of moisture from ocean to land (mm day^{-1}). A 12-month running mean has been added. To compare units, the area of the globe (0.51), ocean (0.36), and land (0.15) $\times$ 10^{15} m^2 must be factored into the units, and the ocean factor applies to the bottom panel.

highest is R1, which results from the unduly smoothed and low topography of Antarctica at T62 resolution.

For the reanalyses, the values from all islands such as New Zealand, Japan, Madagascar, the United Kingdom, and so on amount to 1.0–1.3 ($\times 10^3$ km^3 yr^{-1}). Table 3 lists the reanalyses contributions from Indonesia, Greenland, and Antarctica. The sum of the values are given, and the $\sim 7 \times 10^3$ km^3 yr^{-1} contributed by Indonesia, Antarctica, and the islands makes up most of the difference with the total from Fig. 1 given in the last line for T07. Even allowing for the differences in islands included, the values from reanalyses are a bit low for Eurasia, but high for South America. For Australia, ERA-I is actually negative, as was ERA-40, apparently because of excess evaporation. This accounts for some of the deficiency in ERA-I in the global total.

For North America, the runoff values from Dai and Trenberth (2002) were 6.6×10^3 km^3 yr^{-1} as the net climatological flow into the ocean from all rivers plus ungauged areas and including Greenland. The $P - E$ is lower for 1989–2001 versus 2002–08 for North America by 0.09 for MERRA and 0.04 for ERA-I. These aspects will be explored in more detail elsewhere.

The $E - P$ from divergence of moisture transports is much more stable and seems more reliable than the freshwater fluxes in all reanalyses. While they are all slightly low when compared with the observed estimate based upon river discharge, the values for the 2002–08 are well within uncertainties. Nonetheless, the maps (Fig. 7) reveal several locations where values are in error.

5. The global energy budget

The various terms in the global mean energy budget have been computed at the TOA and surface, as well as for the atmosphere (Fig. 10). Large spurious trends occur not only in latent energy fluxes but also in radiation and clouds in MERRA (Bosilovich et al. 2011), and Fig. 10 provides a snapshot for 2002–08. The global mean evaporation and precipitation expressed as energy fluxes show

TABLE 2. The mean convergence of moisture over land expressed as $P - E$ values (mm day^{-1}) for the 1990s for the annual mean and for the mean annual cycle. Values over ocean can be derived by multiplying these values by 0.42 or converted to total transport in units of kilograms per second by multiplying by 1.60×10^9. Values greater than 0.7 mm day^{-1} are in boldface type.

Reanalysis	Annual	Jan	Feb	Mar	Apr	May	Jun	Jul	Aug	Sep	Oct	Nov	Dec
ERA-40	0.70	**0.85**	**0.90**	**0.88**	**0.77**	0.61	0.46	0.51	0.56	0.63	**0.71**	**0.76**	**0.77**
ERA-I	0.56	**0.70**	**0.72**	0.66	0.54	0.40	0.35	0.42	0.50	0.56	0.60	0.62	0.63
JRA	0.50	0.68	**0.70**	0.65	0.54	0.37	0.26	0.30	0.37	0.45	0.53	0.59	0.62
MERRA	0.65	**0.84**	**0.84**	**0.77**	0.68	0.51	0.45	0.53	0.54	0.56	0.65	**0.71**	**0.78**
R1	0.63	**0.81**	**0.82**	0.73	0.57	0.42	0.36	0.39	0.52	**0.64**	**0.74**	**0.77**	**0.76**
CFSR	0.67	**0.89**	**0.92**	**0.85**	**0.72**	0.56	0.41	0.44	0.55	0.57	0.63	**0.70**	**0.80**

the differences from Fig. 9 in a different context. The latent heating (LP) is substantially greater than the surface latent energy flux (LE) for MERRA, ERA-40, CFSR, and C20r, which underscores the untenable nature of the precipitation amounts over ocean, while ERA-I has lower values.

The R1 reanalysis suffers from an excessively high surface albedo over the ocean, which makes the reflected solar component too high, the ASR much too low, and the TOA albedo unduly high, resulting in a net TOA deficit of >-13 W m^{-2} for 2002–08. The earlier reanalyses (R1, R2, and JRA) did not include changing atmospheric composition, such as increases in carbon dioxide or aerosols, adversely affecting their energy budgets. Clouds in reanalyses are all seriously in error (Trenberth and Fasullo 2010). All of the net TOA imbalances are not tenable and all except CFSR imply a cooling of the planet that clearly has not occurred.

Modest differences exist in the prescribed total solar irradiance (Fig. 10), and low albedo in MERRA and JRA leads to excesses in ASR. Evidently a "bug" in the code at ECMWF led to the high values of total solar irradiance for ERA-40 and ERA-I (Dee et al. 2011). JRA and CFSR also have unduly low reflected amounts

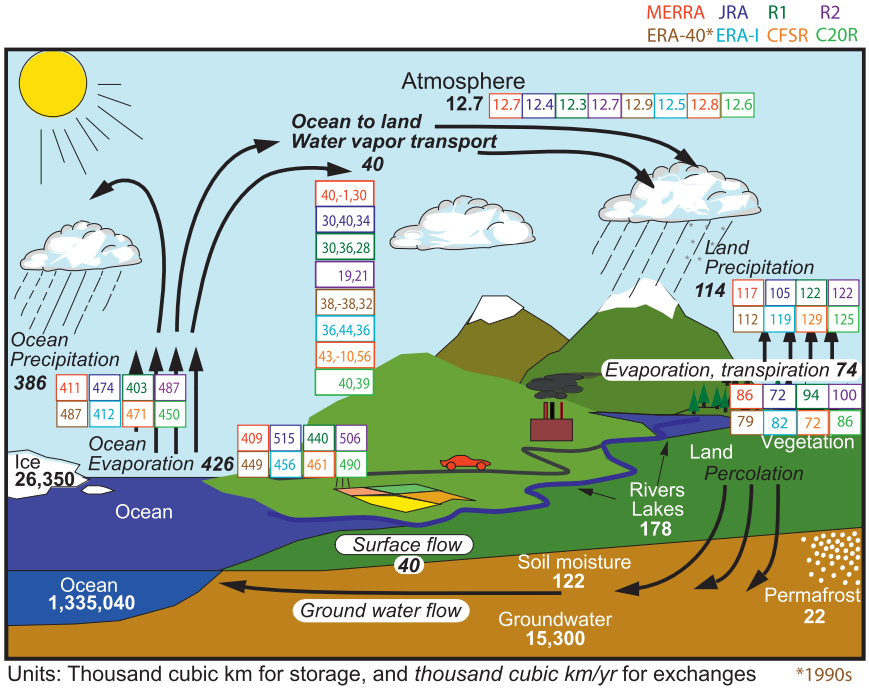

FIG. 9. The background figure shows the estimates of the observed hydrological cycle adjusted from Trenberth et al. (2007b) to apply to the 2002–08 (1000 km^3 for storage and 1000 km^3 yr^{-1} for exchanges). Superposed are values from the eight reanalyses for 2002–08 (color coded as given at the top-right of the panel). The exception is for ERA-40, which is for the 1990s. For the water vapor transport from ocean to land, the three estimates given for each are (i) the actual transport estimated from the moisture budget (based on analyzed winds and moisture), (ii) the $E - P$ from the ocean, and (iii) $P - E$ from the land, which should be identical.

TABLE 3. Regional estimates for land areas for 1979–2007 from T07 for P, E, and $P - E$ as the river discharge into the ocean, and values from moisture transports from the reanalyses MERRA and ERA-I for 2002–08 (Eg yr^{-1}). Values for MERRA and ERA-I are given for contiguous landmasses, and the sum of the identified contributions is given for comparison with the total for all land in the last line.

	From T07 1979–2000			2002–08 $P - E$	
Region	P	E	$P - E$	MERRA	ERA-I
North America	15.3	7.2	8.1	6.3	4.6
South Americal	27.2	18.1	9.1	10.1	11.5
Eurasia	28.8	16.7	12.1	9.8	8.3
Africa	19.2	15.5	4.7	2.9	3.9
Australia	3.8	2.6	1.2	1.7	−0.6
Indonesia				4.2	4.0
Antarctica				2.7	2.2
Greenland				0.9	0.7
Islands				1.3	1.0
Sum	94.3	60.1	34.2	40.1	35.8
Total	107	67	40	40	36

from clouds and the atmosphere. Absorption in the atmosphere is also low for MERRA and R1, indicating that absorption by aerosols and water vapor is likely deficient.

The R2 has a very low surface sensible heat flux and a very high latent heat flux, indicating major problems that have direct consequences for hydrology. OLR is too high in most reanalyses. Most reanalyses are slightly high for surface radiation emissions, which are related to surface temperatures. However, the downwelling longwave radiation at the surface is high for R2, ERA-40, ERA-I, CFSR, and C20r, although there is considerable uncertainty in the observed value. Differences between LE and LP are substantial for MERRA, ERA-40, ERA-I, CFSR, and C20r, again suggesting a considerable contribution from the analysis increment.

The net effect of all these processes and energy flows is the imbalance at the surface, which is unacceptable in all cases. MERRA, C20r, and JRA are out of balance by >10 W m^{-2}, and JRA is strongly negative and of the wrong sign, while ERA-40, ERA-I, CFSR, and C20r are much too high. The difference between the net TOA radiative fluxes and the surface energy fluxes gives the imbalance within the atmosphere of order 10 (range from 4 to 15) W m^{-2}, while observed values must be close to zero as the change in storage in the atmosphere on this time scale is small.

6. Comparison with CCSM4

To complement these water cycle components from reanalyses, we also briefly examine the corresponding

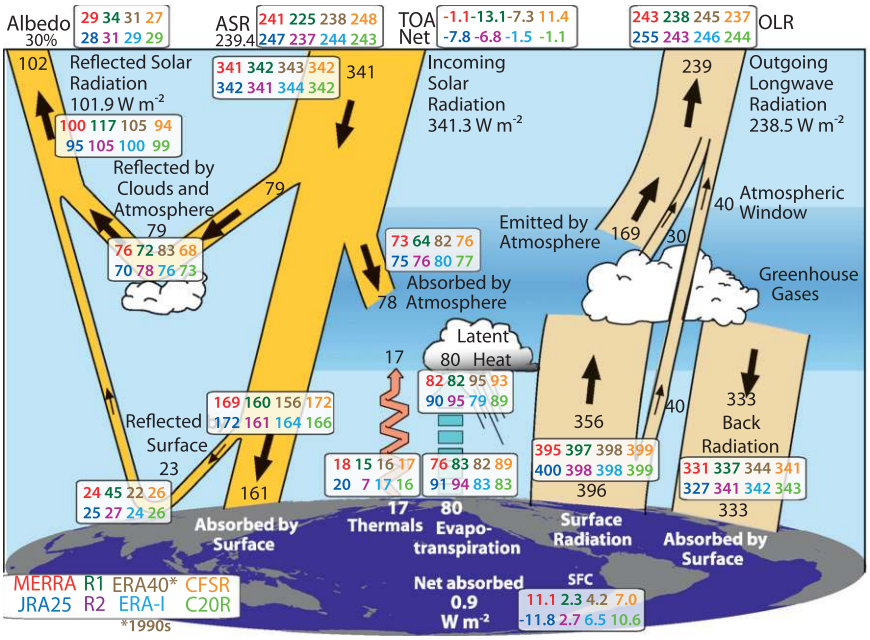

FIG. 10. The background values of radiation or energy flows (Trenberth et al. 2009) are based on observations for 2000–05. Superposed, with the key (lower left), are values from the various reanalyses for the 2002–08 period except for ERA-40, which is for the 1990s (color coded; W m^{-2}). Above the graphic, values are given for albedo (%), ASR, net TOA radiation, and OLR; the box labeled SFC near the bottom gives the net flux absorbed at the surface. For the 1990s the latter value is 0.6 W m^{-2}.

values for version 4 of the NCAR Community Climate System Model (see online at http://www.cesm.ucar.edu/models/ccsm4.0/), which is a fully coupled model running freely under estimated forcings for the twentieth century. An advantage of such a model is that it conserves both energy and water substance and thus provides a contrast to the reanalyses and aids interpretation of results. The model has many new features over the previous version and the atmospheric model resolution is 1°; see Gent et al. (2011) for a description of the model and recent changes implemented as well as a commentary on its performance. There have been five ensemble members made available at the current time, and the variability among them is very small, 1×10^3 km^3 yr^{-1} in all of the quantities examined. For CCSM4 during the 1990s, P-ocean is $419 \pm 1 \times 10^3$ km^3 yr^{-1}, which is over 8% larger than the observed estimate. The E-ocean is 458×10^3 km^3 yr^{-1}, which is also larger than observed, while $E - P$ ocean (40×10^3 km^3 yr^{-1}) is in line with the observed estimate. As the model conserves moisture, this equals the transport from ocean to land and the excess of $P - E$ over land. However, E-land is 91 (vs 74) and P-land is 131 (vs 113). Accordingly, the hydrological cycle is more intense for CCSM4 than the real world, although the transport from ocean to land is reasonable. This is consistent with earlier versions of the model in which precipitation was found to occur prematurely and the lifetime of moisture in the atmosphere was too short (Dai and Trenberth 2004).

Energy constraints provide insight into the source of the anomalously strong hydrologic cycle. Global precipitation in CCSM4 for the 1990s is 2.97 mm day^{-1}, corresponding to 85.8 W m^{-2} latent heating of the atmosphere, considerably larger than the 80 W m^{-2} estimated by Trenberth et al. (2009). Most terms in the energy budget are remarkably similar to those in Trenberth et al., the exception being the downward surface solar radiation, which is 6 W m^{-2} higher. The latter arises mainly from a lower absorption of solar radiation in the atmosphere, presumably associated with aerosols (including black carbon) and water vapor. Hence, the extra energy available at the surface in the model has direct consequences for the overall hydrological cycle.

7. Conclusions

The very nature of the atmospheric reanalyses and their goal of producing time series of the best available analyses, given the observing system, means that they do not conserve quantities that should be conserved from physical principles, and spurious changes occur over time as the observing system changes. While natural variations from year to year are usually large enough that these factors are not very important, it is not always the case, and for decadal climate change or trends the reanalyses have substantial limitations. The reanalyses produce quite good results for precipitation over land but E, P, and $E - P$ over the ocean based on the model output are not stable; they mostly disagree and are unreliable, violate basic physical constraints, and probably should only be used after demonstrating their validity.

The low value of $P - E$ on land in most reanalyses (except CSFR and C20r) is consistent with past studies, showing that the lifetime of moisture in models is too short and recycling is too large (Trenberth et al. 2003; Ruiz-Barradas and Nigam 2005) so that the contribution from advection is too low. For CSFR, the moisture for precipitation must come from the analysis increment, but the implication is again that the model prematurely precipitates.

In general the precipitation and evaporation over oceans in reanalysis models, and also CCSM4, are too large with the notable exception of MERRA. The CCSM4 result suggests this is partly from excessive surface heating resulting from insufficient energy absorption within the atmosphere: if this is so, then it relates to water vapor and aerosols. However, for reanalysis models, the energy supply is less an issue as the SSTs are specified; hence, the errors relate to excessive evaporation (except in MERRA). Chronically premature precipitation from models (e.g., Trenberth et al. 2003; Dai and Trenberth 2004) provides little reason for faith in the model estimates of P or E, and it is not uncommon for the balance to be between the analysis increment (instead of E) and precipitation in wet areas, or E and the analysis increment in dry regions (e.g., where the soil moisture has been specified incorrectly) as seems likely over Australia, for instance, for ERA-40 (see T07) and also ERA-I.

Previously we found that the atmospheric moisture budget generally provides a better estimate of the hydrological cycle components (Trenberth and Guillemot 1998; T07); and this finding still holds with the latest reanalyses. Indeed, $E - P$ from the moisture budget is considerably more stable in time and consistent across the reanalyses. Thus, our observational best estimates of the energy and water budgets and components of the hydrological cycle generally provide a key test of the fidelity of both the reanalyses and climate models. The results also inform our knowledge about $E - P$.

Acknowledgments. We thank Mike Bosilovich and Dick Dee for comments. This research is partially sponsored by NASA Grant NNX09AH89G and NOAA under Grant NA07OAR4310051.

APPENDIX

List of Acronyms

AIRS	Atmospheric Infrared Sounder
AMSU-B	Advanced Microwave Sounding Unit-B
ASR	Absorbed solar radiation
ATOVS	Advanced TOVS
C20r	Twentieth-Century Reanalysis
CCSM	Community Climate System Model
CFS	Climate Forecast System
CFSR	CFS Reanalysis
CMAP	NOAA Climate Prediction Center Merged Analysis of Precipitation
COSMIC	Constellation Observing System for Meteorology, Ionosphere, and Climate
DMSP	Defense Meteorological Satellite Program
DOE	U.S. Department of Energy
ECMWF	European Centre for Medium Range Weather Forecasts
ERA-40	ECWMF 40-yr Reanalysis
ERA-I	ECMWF Interim Reanalysis
ET	Evapotranspiration
GEOS	Goddard Earth Observing System
GPCP	Global Precipitation Climatology Project
GPS	Global Positioning System
GRACE	Gravity Recovery and Climate Experiment
GSSTF	Goddard Satellite-Based Surface Turbulent Fluxes
HOAPS	Hamburg Ocean–Atmosphere Parameters and Fluxes from Satellite Data
IPCC	Intergovernmental Panel on Climate Change
JMA	Japan Meteorological Agency
JRA	Japanese Reanalysis
MERRA	Modern-Era Retrospective-Analysis for Research and Applications
MSAP	Multisource Analysis of Precipitation
NASA	National Aeronautics and Space Administration
NCAR	National Center for Atmospheric Research
NCEP	National Centers for Environmental Prediction
NOAA	National Oceanic and Atmospheric Administration
NOC	National Oceanographic Centre, Southampton
OAFlux	Ocean–Atmosphere Flux
OLR	Outgoing Longwave Radiation
PR	Precipitation radar
R1	NCEP–NCAR reanalysis
R2	NCEP–DOE reanalysis
RO	Radio Occultation
SSM/I	Special Sensor Microwave Imager
SST	Sea Surface Temperature
TIROS	Television and Infrared Observation Satellite
TMI	TRMM Microwave Imager
TOA	Top of atmosphere
TOVS	TIROS Operational Vertical Sounder
TRMM	Tropical Rainfall Measuring Mission

REFERENCES

Adler, R. F., C. Kidd, G. Petty, M. Morrissey, and H. Goodman, 2001: Intercomparison of global precipitation products: The Third Precipitation Intercomparison Project (PIP-3). *Bull. Amer. Meteor. Soc.,* **82,** 1377–1396.

——, and Coauthors, 2003: The version-2 Global Precipitation Climatology Project (GPCP) monthly precipitation analysis (1979–present). *J. Hydrometeor.,* **4,** 1147–1167.

Berry, D. I., and E. C. Kent, 2009: A new air–sea interaction gridded dataset from ICOADS with uncertainty estimates. *Bull. Amer. Meteor. Soc.,* **90,** 645–656.

——, and ——, 2011: Air-sea fluxes from ICOADS: The construction of a new gridded dataset with uncertainty estimates. *Int. J. Climatol.,* **31,** 987–1001, doi:10.1002/joc.2059.

Bloom, S. C., L. L. Takacs, A. M. da Silva, and D. Ledvina, 1996: Data assimilation using incremental analysis updates. *Mon. Wea. Rev.,* **124,** 1256–1271.

Bosilovich, M. G., and Coauthors, 2006: NASA's Modern Era Retrospective-analysis for Research and Applications (MERRA). *U.S. CLIVAR Variations,* Vol. 4, No. 2, 5–8. [Available online at http://www.usclivar.org/Newsletter/Variations_V4N2/CLIVAR%20NL%20MERRA.pdf.]

——, J. Chen, F. R. Robertson, and R. F. Adler, 2008: Evaluation of global precipitation in reanalyses. *J. Appl. Meteor. Climatol.,* **47,** 2279–2299.

——, F. R. Robertson, and J. Chen, 2011: Global energy and water budgets in MERRA. *J. Climate,* in press.

Chou, S. H., E. Nelkin, J. Ardizzone, R. M. Atlas, and C. L. Shie, 2003: Surface turbulent heat and momentum fluxes over global oceans based on the Goddard Satellite retrievals, version 2 (GSSTF2). *J. Climate,* **16,** 3256–3273.

——, ——, ——, and ——, 2004: A comparison of latent heat fluxes over global oceans for four flux products. *J. Climate,* **17,** 3973–3989.

Compo, G. P., and Coauthors, 2011: The Twentieth Century Reanalysis Project. *Quart. J. Roy. Meteor. Soc.,* **137,** 1–28.

Dai, A., and K. E. Trenberth, 2002: Estimates of freshwater discharge from continents: Latitudinal and seasonal variations. *J. Hydrometeor.,* **3,** 660–687.

——, and ——, 2004: The diurnal cycle and its depiction in the Community Climate System Model. *J. Climate,* **17,** 930–951.

——, T. Qian, K. E. Trenberth, and J. D. Milliman, 2009: Changes in continental freshwater discharge from 1949 to 2004. *J. Climate,* **22,** 2773–2791.

——, J. Wang, P. W. Thorne, D. E. Parker, L. Haimberger, and X. L. Wang, 2011: A new approach to homogenize radiosonde humidity data. *J. Climate,* **24,** 965–991.

Dee, D., and S. Uppala, 2009: Variational bias correction of satellite radiance data in the ERA-Interim reanalysis. *Quart. J. Roy. Meteor. Soc.,* **135,** 1830–1841.

——, and Coauthors, 2011: The ERA-Interim reanalysis: Configuration and performance of the data assimilation system. *Quart. J. Roy. Meteor. Soc.,* **137,** 553–597.

Gent, P. R., and Coauthors, 2011: The Community Climate System Model version 4. *J. Climate,* in press.

Grist, J. P., and S. A. Josey, 2003: Inverse analysis adjustment of the SOC air–sea flux climatology using ocean heat transport constraints. *J. Climate,* **16,** 3274–3295.

Gu, G., R. F. Adler, G. J. Huffman, and S. Curtis, 2007: Tropical rainfall variability on interannual-to-interdecadal and longer time scales derived from the GPCP monthly product. *J. Climate,* **20,** 4033–4046.

Huffman, G. J., R. F. Adler, D. T. Bolvin, and G. Gu, 2009: Improving the global precipitation record: GPCP version 2.1. *Geophys. Res. Lett.,* **36,** L17808, doi:10.1029/2009GL040000.

Jiang, C., M. F. Cronin, K. A. Kelly, and L. Thompson, 2005: Evaluation of a hybrid satellite- and NWP-based turbulent heat flux product using the Tropical Atmosphere-Ocean (TAO) buoys. *J. Geophys. Res.,* **110,** C09007, doi:10.1029/2004JC002824.

Josey, S. A., E. C. Kent, and P. K. Taylor, 1999: New insights into the ocean heat budget closure problem from analysis of the SOC air–sea flux climatology. *J. Climate,* **12,** 2856–2880.

Jung, M., and Coauthors, 2010: Recent decline in the global land evapotranspiration trend due to limited moisture supply. *Nature,* **467,** 951–954.

Kalnay, E., and Coauthors, 1996: The NCEP/NCAR 40-Year Reanalysis Project. *Bull. Amer. Meteor. Soc.,* **77,** 437–472.

Kanamitsu, M., W. Ebisuzaki, J. Woollen, S.-K. Yang, J. J. Hnilo, M. Fiorino, and G. L. Potter, 2002: NCEP-DOE AMIP-II Reanalysis (R-2). *Bull. Amer. Meteor. Soc.,* **83,** 1631–1643.

Large, W. G., and S. G. Yeager, 2009: The global climatology of an interannually varying air-sea flux data set. *Climate Dyn.,* **33,** 341–364.

Oki, T., and S. Kanae, 2006: Global hydrological cycles and world water resources. *Science,* **313,** 1068–1072.

Onogi, K., and Coauthors, 2007: The JRA-25 Reanalysis. *J. Meteor. Soc. Japan,* **85,** 369–432.

Robertson, F. R., D. E. Fitzjarrald, and C. D. Kummerow, 2003: Effects of uncertainty in TRMM precipitation radar path integrated attenuation on interannual variations of tropical oceanic rainfall. *Geophys. Res. Lett.,* **30,** 1180, doi:10.1029/2002GL016416.

Rosen, R. D., and A. S. Omolayo, 1981: Exchange of water vapor between land and ocean in the Northern Hemisphere. *J. Geophys. Res.,* **86,** 12 147–12 152.

Ruiz-Barradas, A., and S. Nigam, 2005: Warm season rainfall variability over the U.S. Great Plains in observations, NCEP and ERA-40 reanalyses, and NCAR and NASA atmospheric model simulations. *J. Climate,* **18,** 1808–1830.

Saha, S., and Coauthors, 2010: The NCEP Climate Forecast System Reanalysis. *Bull. Amer. Meteor. Soc.,* **91,** 1015–1057.

Sapiano, M. R. P., T. M. Smith, and P. A. Arkin, 2008: A new merged analysis of precipitation utilizing satellite and reanalysis data. *J. Geophys. Res.,* **113,** D22103, doi:10.1029/2008JD010310.

Schlosser, C. A., and P. R. Houser, 2007: Assessing a satellite-era perspective of the global water cycle. *J. Climate,* **20,** 1316–1338.

Simmons, A., S. Uppala, D. Dee, and S. Kobayashi, 2007: ERA-Interim: New ECMWF reanalysis products from 1989 onwards. *ECMWF Newsletter,* No. 110, ECMWF, Reading, United Kingdom, 25–35. [Available online at http://www.ecmwf.int/publications/newsletters/pdf/110_rev.pdf.]

——, K. M. Willett, P. D. Jones, P. W. Thorne, and D. P. Dee, 2010: Low-frequency variations in surface atmospheric humidity, temperature, and precipitation: Inferences from reanalyses and monthly gridded observational data sets. *J. Geophys. Res.,* **115,** D01110, doi:10.1029/2009JD012442.

Smith, S. R., D. M. Legler, and K. V. Verzone, 2001: Quantifying uncertainties in NCEP reanalyses using high-quality research vessel observations. *J. Climate,* **14,** 4062–4072.

Smith, T. M., M. R. P. Sapiano, and P. A. Arkin, 2008: Historical reconstruction of monthly oceanic precipitation (1900-2006). *J. Geophys. Res.,* **113,** D17115, doi:10.1029/2008JD009851.

Stephens, G. L., and J. M. Haynes, 2007: Near global observations of the warm rain coalescence process. *Geophys. Res. Lett.,* **34,** L20805, doi:10.1029/2007GL030259.

Sterl, A., 2004: On the (in)homogeneity of reanalysis products. *J. Climate,* **17,** 3866–3873.

Sturaro, G., 2003: A closer look at the climatological discontinuities present in the NCEP/NCAR reanalysis temperature due to the introduction of satellite data. *Climate Dyn.,* **21,** 309–316.

Syed, T. H., J. S. Famiglietti, and D. P. Chambers, 2009: GRACE-based estimates of terrestrial freshwater discharge from basin to continental scales. *J. Hydrometeor.,* **10,** 22–40.

——, ——, ——, J. K. Willis, and K. Hilburn, 2010: Satellite-based global-ocean mass balance estimates of interannual variability and emerging trends in continental freshwater discharge. *Proc. Natl. Acad. Sci. USA,* **42,** 17 916–17 921, doi:10.1073/pnas.1003292107.

Trenberth, K. E., 2009: An imperative for climate change planning: Tracking Earth's global energy. *Curr. Opinion Environ. Sustain.,* **1,** 19–27, doi:10.1016/j.cosust.2009.06.001.

——, 2011: Changes in precipitation with climate change. *Climate Res.,* **47,** 123–138.

——, and C. J. Guillemot, 1998: Evaluation of the atmospheric moisture and hydrological cycle in the NCEP/NCAR reanalyses. *Climate Dyn.,* **14,** 213–231.

——, and A. Dai, 2007: Effects of Mount Pinatubo volcanic eruption on the hydrological cycle as an analog of geoengineering. *Geophys. Res. Lett.,* **34,** L15702, doi:10.1029/2007GL030524.

——, and J. T. Fasullo, 2010: Simulation of present-day and twenty-first-century energy budgets of the Southern Oceans. *J. Climate,* **23,** 440–454.

——, D. P. Stepaniak, and J. M. Caron, 2002: Accuracy of atmospheric energy budgets from analyses. *J. Climate,* **15,** 3343–3360.

——, A. Dai, R. M. Rasmussen, and D. B. Parsons, 2003: The changing character of precipitation. *Bull. Amer. Meteor. Soc.,* **84,** 1205–1217.

——, J. Fasullo, and L. Smith, 2005: Trends and variability in column-integrated water vapor. *Climate Dyn.,* **24,** 741–758.

——, and Coauthors, 2007a: Observations: Surface and atmospheric climate change. *Climate Change 2007: The Physical Sciences Basis*, S. Solomon et al., Eds., Cambridge University Press, 235–336.

——, L. Smith, T. Qian, A. Dai, and J. Fasullo, 2007b: Estimates of the global water budget and its annual cycle using observational and model data. *J. Hydrometeor.,* **8,** 758–769.

——, J. T. Fasullo, and J. Kiehl, 2009: Earth's global energy budget. *Bull. Amer. Meteor. Soc.,* **90,** 311–323.

——, and Coauthors, 2011: Atmospheric reanalyses: A major resource for ocean product development and modeling. *Proc. OceanObs'09: Sustained Ocean Observations and Information for Society Conf.,* Vol. 2, ESA Publ. WPP-306, Venice, Italy, ESA, 8 pp. [Available online at http://www.oceanobs09.net/proceedings/cwp/Trenberth-OceanObs09.cwp.90.pdf.]

Uppala, S. M., and Coauthors, 2005: The ERA-40 Reanalysis. *Quart. J. Roy. Meteor. Soc.,* **131,** 2961–3012.

van der Ent, R. J., H. H. G. Savenije, B. Schaefli, and S. C. Steele-Dunne, 2010: Origin and fate of atmospheric moisture over continents. *Water Resour. Res.,* **46,** W09525, doi:10.1029/2010WR009127.

Wentz, F. J., L. Ricciardulli, K. Hilburn, and C. Mears, 2007: How much more rain will global warming bring? *Science,* **317,** 233–235.

Xie, P., and P. A. Arkin, 1997: Global precipitation: A 17-year monthly analysis based on gauge observations, satellite estimates, and numerical model outputs. *Bull. Amer. Meteor. Soc.,* **78,** 2539–2558.

Yin, X., A. Gruber, and P. Arkin, 2004: Comparison of the GPCP and CMAP merged gauge–satellite monthly precipitation products for the period 1979–2001. *J. Hydrometeor.,* **5,** 1207–1222.

Yu, L. S., and R. A. Weller, 2007: Objectively analyzed air–sea heat fluxes for the global ice-free oceans (1981–2005). *Bull. Amer. Meteor. Soc.,* **88,** 527–539.